

# Molecular modeling used as a Probe of Interactions to study the polymeric glass transition

Armand Soldera<sup>a</sup>

<sup>a</sup>Département de Chimie, Université de Sherbrooke, Sherbrooke (Québec), J1K 2R1

Poly(methyl methacrylate), PMMA, exhibits different glass transition temperatures,  $T_g$ s, according to the configuration of its chain. Consequently, molecular modeling offers an ideal tool to understand from molecular interactions the reasons that give rise to such a difference, and as a matter of fact, to better understand the tricky problem of glass transition. However, an intimately link has to be completed with experience, theory, and actual computing resources, to give an accurate interpretation. Differences between the two configurations were then observed from variation of the non-bond energy, intra-diad angle and the local dynamics. More specifically, a different coupling is observed between the side-chain and the backbone. All these differences tend to explain the reason for a variation in  $T_g$ s.

*Le poly(méthyle méthacrylate), PMMA, offre la particularité de présenter une température de transition vitreuse,  $T_g$ , différente selon la tacticité de sa chaîne. De ce fait, la modélisation moléculaire est un outil de choix pour tenter de comprendre à partir des seules interactions moléculaires, les raisons d'une telle différence, et de ce fait, de mieux appréhender le délicat problème de la transition vitreuse. Toutefois, une utilisation concertée de la modélisation moléculaire avec les résultats expérimentaux, théoriques, et les ressources informatiques, est nécessaire afin de donner une interprétation cohérente du phénomène. Des différences entre les deux configurations du PMMA ont ainsi pu être constatées dans les termes d'énergie intermoléculaire, dans l'angle intra-diade et au sein de la dynamique locale. Plus spécifiquement, une coopérativité différente est constatée entre la chaîne latérale et le squelette. Toutes ces différences contribuent à une meilleure compréhension de la variation de  $T_g$ .*

Molecular modeling is playing an increasing role in a laboratory since it grants insight into the factors that give rise to specific properties, and thus it both helps to the understanding of molecular phenomena, and guides the synthesis of new compounds with enhanced properties. Actually, it could highlight microscopic behavior that experimental techniques could not deal with. However, accuracy of the simulation obviously stems from appropriate models and computer resources. If they are suitably employed, they could shed light on tricky problems in polymer science, such as the glass transition.

The glass transition temperature,  $T_g$ , is of great importance in polymer applications since it splits apart two domains of different mechanical behaviors. Below  $T_g$ , the material exhibits high Young's modulus, and above  $T_g$ , it displays elastic properties. Different theories, free volume<sup>1</sup>, kinetics<sup>2</sup> and thermodynamics<sup>3</sup>, try to explain such a transition. With the help of molecular modeling, microscopic behavior could be revealed. However, this procedure has to follow a methodology based on perpetual interaction with experimental and theoretical results.

Poly(methyl methacrylate), PMMA, whose repeat unit is displayed in figure 1, presents a specific regard on the understanding of the glass transition: according to the alternation of its side-chain (C(O)OCH<sub>3</sub>), a different  $T_g$  is obtained. Consequently, this variation might be interpreted in terms of changes in molecular characteristics that can be investigated by molecular modeling.

## Initial Parameters

Due to the great number of atoms in polymers, empirical methods, molecular mechanics and dynamics, are usually

employed. They are based on the use of a force field<sup>4</sup>. A force field expresses the interaction between atoms considering the electronic interactions in average. A sum of analytical functions tend to represent these interactions, they are actual mathematical translations of specific interactions: for instance the stretching energy term is usually represented by an harmonic function, or a Morse function, etc ... Depending on the quality of the force field, numerous terms can be added such as the cross terms, yielding to a greater transferability between compounds, and to a better accuracy of the results. Nevertheless, it involves an increase in the computational time. Moreover, each function presents adjustable parameters. They stem from the fit of the function to experimental data or theoretical curves. Since one atom can be surrounded by different electronic environment, numerous fitting parameters can exist for one atom. Consequently, greater is the number of these descriptors for one atom, better is the transferability. The force field used in the glass transition study is pccff from Accelrys: it exhibits a great transferability and was specifically designed to represent interactions among polymers. Its mathematical form is presented in the appendix.

Once the force field is selected the simulation of the amorphous phase of a polymer has to be undertaken. Due to the great number of atoms, the configurational space cannot be covered: the ergodic hypothesis is not satisfied. Nevertheless, statistical rules exist to compute physical properties that are in agreement with experimental data<sup>5</sup>. The problem lies in the fact that simulations are carried out on a low number of chains. Consequently, the region of the configurational space has to be properly selected. This can actually be done by, firstly, performing a generation procedure based on the Self-Avoiding-Walk<sup>6</sup>; secondly,

building a cubic cell whose volume is in agreement with the knowledge of the density and the mass of the polymer; thirdly, imposing the periodic limit conditions<sup>7</sup>; lastly, optimizing the cell containing the polymer. A number of 20-30 initial configurations is usually necessary to represent the phase space of a polymer.

## Molecular Modeling Techniques

Molecular dynamics integrates the equation of motion to give a movement to the atoms, and thus to get a trajectory that can be latter handled. The customary integration algorithm is the Verlet-leapfrog algorithm since it is simplectic (reversible in time), stable, and requires a high integration step, in order of 1 fs. This integration is performed on the microcanonic ensemble to conserve the energy. To use such equation in another ensemble, such as NPT (number of atoms, temperature and pressure are kept constant), algorithms have to be used. To control the temperature, the Nose-Hoover algorithm was used<sup>8,9</sup>, and to control the pressure, it was the Parrinello-Rahman algorithm<sup>10</sup>.

Two kinds of software were employed: Discover\_3© from Accelrys, and DL\_POLY<sup>11</sup>.

## T<sub>g</sub> Determination

Using the NPT ensemble at one temperature and one pressure, the energy and the volume vary until equilibrium is reached. Since the volume is directly related to the density,  $\rho$ , the inverse of the specific volume, a graph with the specific volume versus the temperature can be obtained. Such a technique is analogous to the experimental dilatometry<sup>12</sup>. This procedure was applied to PMMA<sup>13</sup> with a time duration for a molecular dynamics simulation of 100 ps for each specific volume value. From a simulated dilatometry experiment<sup>13</sup>, the difference between the two T<sub>g</sub>s is 55 °C, which is in good agreement with the experimental one, 69 °C. Consequently, further analysis can be carried out. Specific programs have been developed to correctly picture the physical properties. Moreover, configurations at different temperatures have been selected and submitted to simulation of 1 ns. As a result, the averages are more accurate, and the precision in longer times of the time autocorrelation functions is increased.

## Results and Discussion

Local molecular motions constitute the basic process of many physical phenomena such as the glass transition. To establish the link between chemical structure and the local dynamics, molecular dynamics simulation fits perfectly. However, relevant parameters have to be extracted from

trajectories. These parameters are the differences in energy<sup>13</sup>, in geometrical factor<sup>14</sup>, and in time correlation<sup>15</sup>.

Differences in energy

A difference in the non-bond energy was observed. The major contribution comes from s-PMMA (syndiotactic PMMA where the side-chains alternate along the backbone chain) which exhibits the highest T<sub>g</sub>. This result is in accordance with the free volume theory since higher interactions between neighboring chains give a higher T<sub>g</sub>: greater are the interchain interactions, greater is the thermal energy brought to the system for the phenomenon to occur, hence greater is the T<sub>g</sub>. A difference was also observed in the bending angle energy, which was due to a difference in the intra-diad bending angle,  $\theta'$  (figure 1).

Difference in the intra-diad bending angle

i-PMMA (isotactic PMMA where the side-chains are in the same side along the backbone chain) which exhibits the lowest T<sub>g</sub>, presents an intra-diad angle 1 deg. higher than in the case of s-PMMA. Such a difference is due to a greater interaction between the side-chains. As a result, a greater mobility of those side-chains was observed<sup>14</sup>.

1. Computation of the correlation times<sup>15</sup>

The normalized autocorrelation bond vector function of the vector  $\mathbf{u}$ ,  $\langle \mathbf{u}(t) \cdot \mathbf{u}(0) \rangle$ , gives insight into the local dynamics of the motion associated with the bond vector,  $\mathbf{u}$ . It directly stems from a molecular dynamics trajectory. It could then allow the computation of the second Legendre polynomial term:

$$P_2(t) = \frac{1}{2} \left[ 3 \langle (\mathbf{u}(t) \cdot \mathbf{u}(0))^2 \rangle - 1 \right]$$

Actually  $P_2(t)$  expresses the decorrelation of the bond vector  $\mathbf{u}$ . It thus yields to a correlation time. Since the motion of the bond vector is not isotropic, the decorrelation cannot be fitted with a simple exponential.

The usual fitted function is a stretching exponential function, or a Kolrausch-Williams-Watt (KWW) function,

$$\phi(t) = \exp \left[ - (t/\tau)^{\beta_{\text{KWW}}} \right].$$

The use of this stretching function directly yields to the correlation time since it substitutes  $P_2(t)$  in the integral from 0 to infinity. Consequently, the correlation time is:

$$\tau_c = \frac{\tau}{\beta_{\text{KWW}}} \Gamma \left( \frac{1}{\beta_{\text{KWW}}} \right)$$

$\tau$  and  $\beta_{\text{KWW}}$  are adjustable parameters. The physical significance of  $\beta_{\text{KWW}}$  will be outlined in the discussion part. This procedure was carried out at different temperatures, and thus correlation times can be obtained for the two PMMA configurations and for different bond vectors. They are then fitted using the VFT equation:

$$\tau_c(T) = A \exp \left( \frac{B}{T - T_o} \right)$$

$T_o$  is the temperature at which the configurational entropy vanishes.  $B$  can be related to the apparent activation energy. It is not a real activation energy since the equation does not represent an Arrhenius behavior. It has to be pointed out that the Williams-Landel-Ferry (WLF) equation is similar to the VFT equation. The apparent activation energy is then  $2.303RC_1^g C_2^g$ <sup>16</sup>.

The two bond vectors used to compute correlation time are displayed in figure 1.  $\vec{u}_{CH}$  represents the local motion associated with the backbone, and  $\vec{u}_{CO}$  actually displays three motions: the librational motion (eliminated by the use of the stretching function), the motion due to the side-chain, and the motion due to the backbone. The two latter motions cannot be easily separated. Nevertheless, their computation allows to determine the coupling that could exist between the side-chain and the backbone. Actually, this cooperativity is described by the stretching function exponent,  $\beta_{kww}$ <sup>17</sup>. A near unity exponent describes a "strong liquid" (Arrhenius behavior). As it departs from unity, the polymers become more and more fragile (non-arrhenian behavior of the relaxation time)<sup>18</sup>. The knowledge of this exponent is thus a key to exploring the coupling behavior of the motion it refers to.

In figure 2, are presented the behavior of  $\beta_{kww}$  associated with  $\vec{u}_{CH}$ , with respect to the inverse of the relative temperature, for both PMMA configurations. No significant difference is observed. Actually this is reflected in the value of the apparent activation energy  $B$  in the VFT equation: 11.8 kJ.mol<sup>-1</sup> for s-PMMA, and 12.5 kJ.mol<sup>-1</sup> for i-PMMA<sup>15</sup>. Consequently, at a relative temperature above  $T_g$ , both backbone dynamics are similar. The difference stays in the absolute temperature since the  $T_g$  of i-PMMA is lower than the  $T_g$  of s-PMMA.

Figure 3 shows the difference in the  $\beta_{kww}$  behavior associated with  $\vec{u}_{CO}$  for the two configurations with respect to the inverse of the relative temperature. Actually, the apparent activation energies,  $B$  in the VFT equation, are different according to the chain configuration: 11.5 kJ.mol<sup>-1</sup> for s-PMMA, and 5 kJ.mol<sup>-1</sup> for i-PMMA<sup>15</sup>. Consequently, at a temperature higher than  $T_g$ , the two configurations exhibit different behavior. To accurately compare the two polymers, backbone and side-chains have to be very mobile. In this case, the two correlation times are comparable. At high temperatures, the two correlation times overlapped. Consequently, the Kolrausch coefficient,  $\beta_{kww}$ , really unveils the coupling between the backbone and the side-chain. As  $\beta_{kww}$  of i-PMMA is lower than  $\beta_{kww}$  of s-PMMA, a greater cooperativity between the side-chain and the backbone exists in i-PMMA. Such a correlation affects most the mobility of the backbone and consequently, decreases the  $T_g$

according to the free volume theory. It has to be pointed out that intramolecular coupling between the side-chain and the backbone motions have been observed experimentally by Kuebler et al, by comparing PMMA with PEMA (an ethyl group is substituted to the methyl group of the side-chain). The distinction between the two PMMA configurations was not investigated. Molecular modeling is thus complementary to experimental data, and due to the good agreement, it can be used to probe the differences between specific polymers.

In conclusion, the variation of the  $T_g$  between the two PMMA configurations stems from a different behavior of the side-chain. A greater mobility of the side-chain in i-PMMA, in accordance with a greater intra-diad angle, involves a greater mobility of the backbone due to the coupling between the two chains. This behavior results in a  $T_g$  lower for i-PMMA since the backbone chain is more mobile. A concerted use of computer resources, models, experimental data and theories, enabled to better understand the difference in the glass transition temperatures between the two PMMA configurations. However, investigations have to be pursued to fit our results with the mode coupling theory, to the particular thermal behavior of PMMA confined in thin film, ...

## Acknowledgment

Financial support of this work from Université de Sherbrooke is gratefully acknowledged.

## Appendix

### Potential Energy Expression

$$\begin{aligned}
 V = & \sum_b [K_2(b-b_0)^2 + K_3(b-b_0)^3 + K_4(b-b_0)^4] + \sum_\theta [H_2(\theta-\theta_0)^2 + H_3(\theta-\theta_0)^3 + H_4(\theta-\theta_0)^4] \\
 & + \sum_\phi [V_1[1-\cos(\phi-\phi^0)] + V_2[1-\cos(2\phi-\phi^0)] + V_3[1-\cos(3\phi-\phi^0)]] + \sum_x K_x \mathcal{X}^2 \\
 & + \sum_b \sum_b F_{bb}(b-b_0)(b-b_0) + \sum_\theta \sum_\theta F_{\theta\theta}(\theta-\theta_0)(\theta-\theta_0) + \sum_b \sum_b F_{bb}(b-b_0)(\theta-\theta_0) \\
 & + \sum_b \sum_\phi (b-b_0)[V_1 \cos \phi + V_2 \cos 2\phi + V_3 \cos 3\phi] + \sum_b \sum_\theta (b-b_0)[V_1 \cos \phi + V_2 \cos 2\phi + V_3 \cos 3\phi] \\
 & + \sum_\theta \sum_\theta (\theta-\theta_0)[V_1 \cos \phi + V_2 \cos 2\phi + V_3 \cos 3\phi] + \sum_\theta \sum_\theta K_{\theta\theta\theta} \cos \phi (\theta-\theta_0)(\theta-\theta_0) \\
 & + \sum_{i>j} \frac{q_i q_j}{\epsilon r_{ij}^6} + \sum_{i>j} \left[ \frac{A_{ij}}{r_{ij}^3} - \frac{B_{ij}}{r_{ij}^6} \right]
 \end{aligned}$$

## References

- (1) Rigby, D.; Roe, R.-J. *Macromolecules* **1990**, *23*, 5312-5319.
- (2) Doi, M.; Edwards, S. F. *Theory of Polymer Dynamics*; Clarendon Press: Oxford, 1986.

- (3) Gibbs, J. H.; DiMarzio, S. F. *J. Chem. Phys.* **1958**, 28, 373.
- (4) Burkert, U.; Allinger, N. L. *Molecular Mechanics*; ACS: Washington, 1982; Vol. 177.
- (5) Flory, P. J. *Statistical Mechanics of Chain Molecules*; Hanser Publishers: New York, 1989.
- (6) Theodorou, D. N.; Suter, U. W. *Macromolecules* **1985**, 18, 1467-1478.
- (7) Allen, M. P.; Tildesley, D. J. *Computer Simulation of Liquids*; Clarendon Press: Oxford, 1987.
- (8) Nosé, S. *J. Chem. Phys.* **1984**, 81, 511.
- (9) Hoover, W. G. *Phys. Rev. A* **1985**, 31, 1695.
- (10) Parrinello, M.; Rahman, A. *J. Appl. Phys.* **1981**, 52, 7182.
- (11) DL\_POLY is a package of molecular simulation routines written by W. Smith and T.R. Forester, copyright for the Central Laboratory of the Research Councils, Daresbury Laboratory at Daresbury, Nr. Warrington (1996).
- (12) Rigby, D.; Roe, R. J. *J. Chem. Phys.* **1987**, 87(12), 7285-7292.
- (13) Soldera, A. *Macromol. Symp.* **1998**, 133, 21-32.
- (14) Soldera, A. *Polymer* **2002**, 43, 4269-4275.
- (15) Soldera, A.; Grohens, Y. *Macromolecules* **2002**, 35, 722-726.
- (16) Ferry, J. D. *Viscoelastic Properties of Polymers*; New York, 1970.
- (17) Ngai, K. L. *J. Chem. Phys.* **1998**, 109, 6982-6985.
- (18) Ediger, M. D.; Angell, C. A.; Nagel, S. R. *J. Phys. Chem.* **1996**, 100, 13200-13212.

## Figures

Figure 1: PMMA repeat unit with the two vectors,  $\vec{u}_{CH}$  and  $\vec{u}_{CO}$ , which reveal the backbone and side-chain/backbone local dynamics, respectively

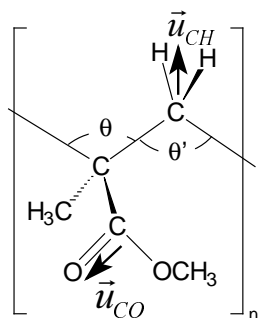


Figure 2: KWW exponent,  $n$ , of the i-PMMA ( $\theta$ ), and s-PMMA ( $\rho$ ) C-H bond vector orientation, with respect to the Tg/T ratio.

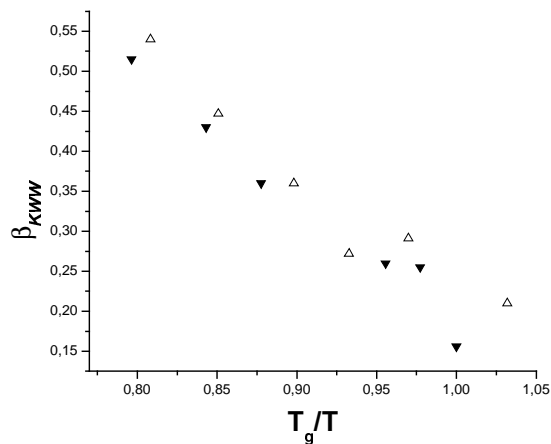


Figure 3: KWW exponent,  $n$ , of the i-PMMA ( $\theta$ ), and s-PMMA ( $\rho$ ) C=O bond vector orientation, with respect to the Tg/T ratio.

